Chem

CellPress

Article

Chemoselective Nitrosylation of Anilines and Alkynes via Fragmentary or Complete NO Incorporation

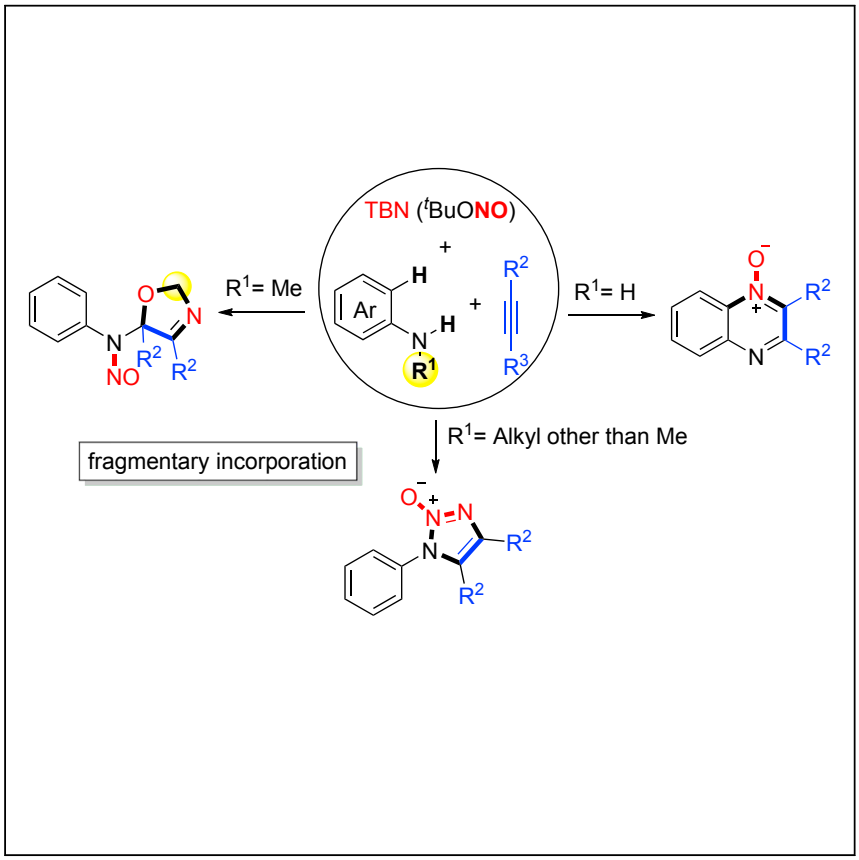

Cycloaddition reactions provide an efficient strategy for the synthesis of cyclic compounds and have been well developed. However, cycloaddition reactions with fragmentary partner incorporation via the cleavage of multiple bonds, which allows for more structural diversity than traditional cycloaddition reactions, have seldom been reported. Here, we describe a chemoselective nitrosylation of anilines and alkynes through fragmentary or complete NO radical incorporation for an efficient approach to 2,5-dihydrooxazoles, 1*H*-1,2,3-triazole 2-oxides, or quinoxaline *N*-oxides.

Jun Pan, Xinyao Li, Fengguirong Lin, Jianzhong Liu, Ning Jiao

jiaoning@pku.edu.cn

HIGHLIGHTS

Fragmentary or complete NO radical incorporation in cycloaddition reactions

A chemoselective nitrosylation of anilines and alkynes

Formation of multiple C–N bonds and an unexpected C–N bond, as well as N=O bond cleavage

Pan et al., Chem 4, 1–16
June 14, 2018
https://doi.org/10.1016/j.chempr.2018.03.008

Please cite this article in press as: Pan et al., Chemoselective Nitrosylation of Anilines and Alkynes via Fragmentary or Complete NO Incorporation, Chem (2018), https://doi.org/10.1016/j.chempr.2018.03.008

Chem

CellPress

Article

Chemoselective Nitrosylation of Anilines and Alkynes via Fragmentary or Complete NO Incorporation

Jun Pan,[1,3] Xinyao Li,[1,3] Fengguirong Lin,[1] Jianzhong Liu,[1] and Ning Jiao[1,2,4,*]

SUMMARY

The cycloaddition reactions have been explored extensively and provided an efficient strategy for the synthesis of cyclic compounds. Traditionally, the reaction partners were *in extenso* incorporated into the cyclic products without fragmentation. From a different perspective, if certain fragmentations via chemical-bond cleavage are involved in this cycloaddition reaction, it would change the assembly sequence and enable more product diversity. Here, we report a chemoselective nitrosylation of anilines and alkynes through fragmentary or complete NO radical incorporation. The formation of multiple C–N bonds, an unexpected C–N bond, and N=O bond cleavage make this fragmentary cycloaddition reaction an efficient approach to 2,5-dihydrooxazoles, 1*H*-1,2,3-triazole 2-oxides or quinoxaline *N*-oxides. Facile operation in open-air, metal-free, and mild conditions renders this protocol particularly practical and attractive. A series of mechanistic studies and density functional theory calculations were also conducted, which help to explain the fragmentary or complete NO incorporation processes, broadening the field of new reaction discovery.

INTRODUCTION

Cycloaddition reactions, including [2 + 2 + 1], [3 + 2 + 1], have been widely used in organic synthesis.[1–6] Traditionally, the reaction partners were completely incorporated into the cyclic products. Theoretically, on the other hand, they might be split into two or more parts and then be fragmentarily incorporated in the cyclic products (Scheme 1A). However, to the best of our knowledge, this kind of fragmentary cycloaddition with reaction partner incorporation via chemical bond cleavage remains unknown. Exploring novel reactions through mechanistic design is universally used by synthetic chemists. Enamine and imine, which can tautomerize to each other, are a class of well-developed intermediates in organic chemistry.[7–11] Although various methodologies involving enamine and imine intermediates have been developed in organic synthesis,[12–18] single-electron oxidation of electron-rich enamine intermediates to trigger radical reactions is still rare despite the high activity of the *in-situ*-generated radical intermediates.[19–22] Recently, reactions through C–H[23–27] and C–C[28–34] cleavage have been powerful strategies for direct transformation of simple substrates. Thus, the combination of a single-electron transfer (SET) process with the generation of very active radical intermediates and C–H/C–C functionalization would potentially open the door to a new field of reaction discovery.

We have been interested in the development of a methodology based on iminium intermediates through a single-electron-transfer (SET) and deprotonation process followed by the capture of O_2 or N_3 radicals.[35–38] Recently, *tert*-butyl nitrite (TBN) has

The Bigger Picture

Exploring novel structures and developing convenient and direct methods to achieve them are an essential issue in synthetic chemistry. In traditional cycloaddition reactions, the reaction partners are *in extenso* incorporated into the cyclic compound products. In contrast, the fragmentary incorporation of the reaction partners via chemical-bond cleavage in cycloaddition reactions would change the assembly sequence and enable more product diversity. However, fragmentary incorporation in cycloaddition reactions remains a challenging issue because of the high bond-dissociation energy and poor selectivity. This paper reports a fragmentary cycloaddition reaction that enables a series of new structures through a controllable radical process. This work also reveals the diversity of transformation of free radical intermediates. The accessible products might also trigger some interest in pharmaceutical science and materials science.

been shown to be a very useful building block as a source of N, NO, or NO_2 for the construction of corresponding N-containing compounds under mild conditions.[39–43] Using substituted *N*-ethylidene-anilines **1** as the substrates, we recently reported an efficient approach to quinoxaline *N*-oxides **2** (Scheme 1B).[44] The proposed reaction mechanism starts with single-electron oxidation and deprotonation of imine substrates to generate methyl imine radical intermediate **A**, which can then be trapped by NO radical to form intermediate **B**, and finally C–H annulation delivers the desired product.

Inspired by this chemistry (Scheme 1B) and the methodologies with tautomerization of enamine and imine intermediates,[12–18] we envisioned that enamines **6**, generated *in situ* from the addition of anilines and alkynes, might be suitable candidates for single-electron oxidation affording the radical intermediates **A** (Scheme 1C). In this way, the previous two-component approach to quinoxaline *N*-oxides could be extended to a three-component one, which would enhance the overall efficiency and extend the substrate scope significantly (Scheme 1C). Moreover, according to the proposed mechanism, we were also curious about what novel transformation might occur if *N*-substituted enamines **7** were used to block the known path (Scheme 1C). In fact, an unexpected 2,5-dihydrooxazole **8** and 1*H*-1,2,3-triazole 2-oxide **9** was obtained from *N*-methyl aniline and other *N*-alkylanilines, which attracted our attention because of the unexpected C–N as well as N=O bond cleavage and rearrangement (Scheme 1C). Here, we report a chemoselective nitrosylation of anilines and alkynes for the efficient construction of 2,5-dihydrooxazoles, 1*H*-1,2,3-triazole 2-oxides, and quinoxaline *N*-oxides through fragmentary or complete NO radical incorporation (Scheme 1C). The formation of multiple C–N bonds, an unexpected C–N bond, and N=O bond cleavage make this chemistry more interesting and meaningful. We carried out a series of mechanistic studies to seek an explanation for this selective skeleton assembly and [3 + 2 + 1] cycloaddition processes. Moreover, this transformation features facile operation in open-air, transition-metal-free, and mild conditions for the preparation of *N*-heterocyclic compounds.

RESULTS AND DISCUSSION

Inspired by the previous strategies using TBN as the building block,[39–44] we initiated our investigation by performing the reaction of aniline **3a** with dimethyl butynedioate (**5a**) in the presence of TBN by using CH_3CN as the solvent (Table 1). To our delight, after the reaction mixture was stirred at 60°C for 15 min, the desired product quinoxaline *N*-oxide **2a**, confirmed by X-ray single-crystal diffraction, was isolated in 76% yield (entry 1; see also Figure S115). To further improve the reactivity, we examined a series of additives, nevertheless no significant enhancement was observed (entry 2; see also Table S1). Lower temperature with longer reaction time resulted in moderate yield of the product (Table 1, entry 3), which indicates the reaction can work well under milder conditions. Gratifyingly, screening of several different solvents increased the yield to 83% at room temperature (Table 1, entries 5–8). Fluorinated solvents seemed to be particularly helpful in this reaction, with hexafluoroisopropanol (HFIP) and trifluoroethanol giving 80% and 83% yield, respectively, which is consistent with their positive effect on reactions where free radicals or cationic species are involved.[45,46] Other NO sources were also examined but only lower efficiencies were observed (see Table S1). Finally, **2a** was obtained in 82% yield under the optimized conditions in CF_3CH_2OH at room temperature (condition A, entry 8).

Activation of the C–N bond has become a hot topic in organic synthesis recently, in which most efforts have focused on the amination transformation.[47–51] However, the utilization of alkyl adjacent to the N atom as the migrant group to participate in

[1]State Key Laboratory of Natural and Biomimetic Drugs, School of Pharmaceutical Sciences, Peking University, 100191 Beijing, China

[2]State Key Laboratory of Elemento-organic Chemistry, Nankai University, Weijin Road 94, Tianjin 300071, China

[3]These authors contributed equally

[4]Lead Contact

*Correspondence: jiaoning@pku.edu.cn

https://doi.org/10.1016/j.chempr.2018.03.008

Please cite this article in press as: Pan et al., Chemoselective Nitrosylation of Anilines and Alkynes via Fragmentary or Complete NO Incorporation, Chem (2018), https://doi.org/10.1016/j.chempr.2018.03.008

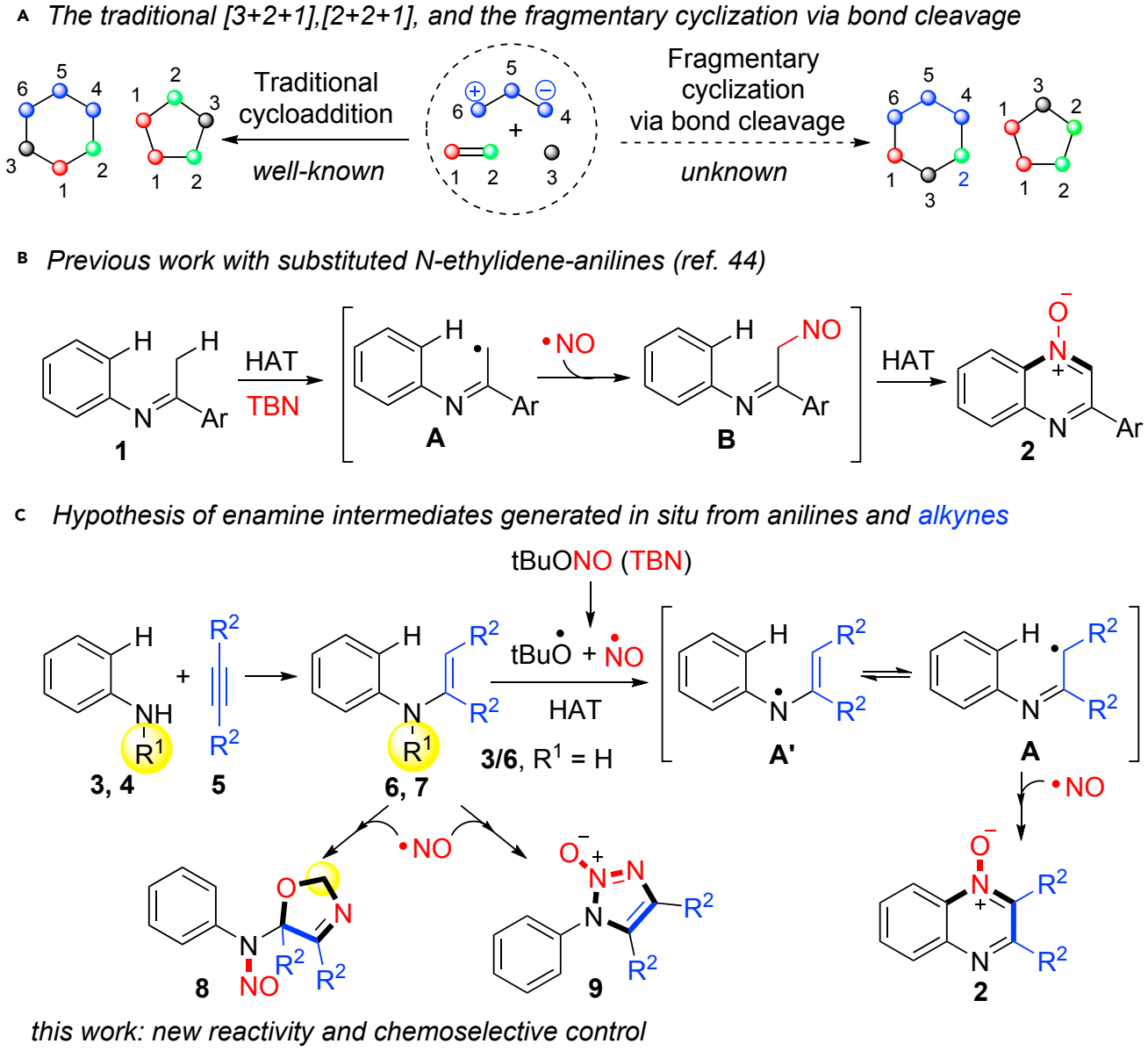

Scheme 1. Cycloaddition of Anilines for the Construction of Heterocycles

annulation has never been achieved. As already mentioned, we wanted to know what would happen with mono-substituted aniline when the pathway discussed above was blocked. Therefore, *N*-methylaniline (**4a**) was subjected to the same conditions as simple aniline. Surprisingly, an unexpected 2,5-dihydrooxazole **8a** was obtained in 37% yield (entry 9), the core ring of which came from three independent components. Increasing the reaction temperature to 60°C for only 15 min increased the yield of **8a** to 52% (entry 10). The use of several additives could not further improve the efficiency (entry 11; see also Table S2). Interestingly, it turned out that HFIP solvent was superior to trifluoroethanol in this case, and other non-fluorinated solvents undermined the reactivity (entries 12–17). Finally, under the optimized conditions in HFIP at 60°C (condition B, entry 17, Table 1), the reaction of *N*-methylaniline (**4a**) produced **8a** in 72% yield.

Please cite this article in press as: Pan et al., Chemoselective Nitrosylation of Anilines and Alkynes via Fragmentary or Complete NO Incorporation, Chem (2018), https://doi.org/10.1016/j.chempr.2018.03.008

Table 1. Optimization for the Reaction of Aniline (3a) and *N*-Methylaniline (4a) with Dimethyl Butynedioate (5a)

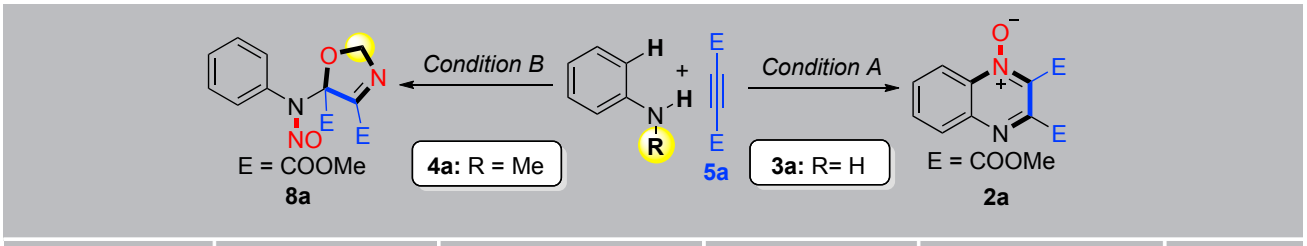

Entry	Aniline	Solvent	*T* (°C)	Time	Yield (%)[a]
1	3a	CH_3CN	60	15 min	2a, 79 (76)
2[b]	3a	CH_3CN	60	15 min	2a, <60
3	3a	CH_3CN	25	overnight	2a, 64
4	3a	toluene	25	overnight	2a, 45
5	3a	DCE	25	overnight	2a, 51
6	3a	THF	25	overnight	2a, 56
7	3a	HFIP	25	overnight	2a, 80 (79)
8	3a	CF_3CH_2OH	25	overnight	2a, 83 (82)
9	4a	CF_3CH_2OH	25	overnight	8a, 38
10	4a	CF_3CH_2OH	60	15 min	8a, 52 (52)
11[c]	4a	CF_3CH_2OH	60	15 min	8a, <52
12	4a	$MeNO_2$	60	15 min	8a, 15
13	4a	1,4-dioxane	60	15 min	8a, 29
14	4a	CH_3CN	60	15 min	8a, 31
15	4a	toluene	60	15 min	8a, 25
16	4a	DCE	60	15 min	8a, 33
17	4a	HFIP	60	15 min	8a, 73 (72)

Reaction conditions: condition A: **3a** (0.5 mmol), **5a** (0.55 mmol), and TBN (3 equiv) in CF_3CH_2OH (1 mL) at 25°C overnight; condition B: **4a** (0.5 mmol), **5a** (0.55 mmol), and TBN (2.2 equiv) in HFIP (1 mL) at 60°C for 15 min. E = CO_2Me.

[a]Yields were determined by ^1H NMR. The numbers in parentheses are isolated yields.

[b]TBAI, KI, and NaBr (0.05 mmol) were used as the additives.

[c]KI, TBAI, Cs_2CO_3, Li_2CO_3, and DBU (0.05–0.1 mmol) were used as the additives.

With the established cycloaddition conditions in hand, we examined the scope of *N*-methylanilines **4** in terms of functional group diversity and substitution pattern under condition B (Figure 1; see also Figures S1–S32). The reaction proved to be tolerant of different substitution patterns on the aromatic core (**8a–8k**). *N*-Methylanilines substituted with the halogens (F, Cl, and Br) afforded the corresponding 2,5-dihydrooxazoles in moderate yields (**8d**–**8f**), which could be used for further functionalization. Phenyl-substituted *N*-methylaniline was smoothly converted into the product **8h**, confirmed by X-ray single-crystal diffraction (see also Figure S114). The unsaturated alkynyl substituent was also tolerated in this transformation (**8l**). Interestingly, 9*H*-fluoren-2-amine smoothly led to the more complex polycyclic compound in moderate yields (**8m**). Diethyl but-2-ynedioate also worked well to afford 2,5-dihydrooxazole in 61% yield (**8n**). Notably, when the methyl group in **4a** was replaced with an ethyl group, the corresponding product **8o** was successfully formed, although in lower yield.

Furthermore, we evaluated the scope and generality of primary anilines **3** in this transformation (Figure 2; see also Figures S33–S74). Substituents at different

Please cite this article in press as: Pan et al., Chemoselective Nitrosylation of Anilines and Alkynes via Fragmentary or Complete NO Incorporation, Chem (2018), https://doi.org/10.1016/j.chempr.2018.03.008

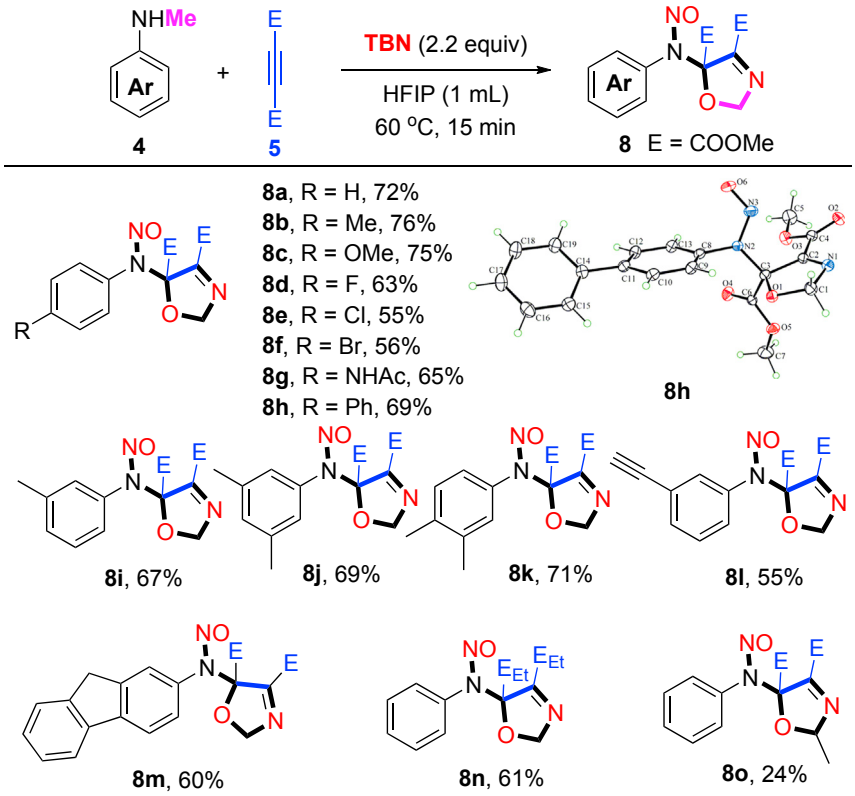

Figure 1. Substrate Scope of *N*-Methylaniline

For the reaction conditions, see entry 17 in Table 1. The yields are isolated yields based on the aniline substrates. E = CO_2Me, E_{Et} = CO_2Et.

positions of the aryl ring of aniline (*para*-, *meta*-, *ortho*-position and multi-substituted) did not undermine the reactivity with good functional group compatibility (**2a–2p**). Halo-substituted anilines were well tolerated, leading to halo-substituted products (**2e–2h**). Electron-donating groups such as alkyl (**2b**, **2m–2o**, **2i**, and **2q**), methoxy (**2c** and **2j**), and benzyloxy (**2k**) were well compatible with this transformation, affording the quinoxaline *N*-oxides in moderate to good yields. The naphthyl-substituted and phenyl-substituted anilines worked well, forming the corresponding quinoxaline *N*-oxides **2q** and **2d**, respectively. The unsaturated group alkynyl was tolerated in this system (**2l**). The morpholinyl substituent that was studied frequently in pharmaceutic sciences was compatible for preparing corresponding quinoxaline *N*-oxide **2r**. Diethyl but-2-ynedioate also worked well to afford quinoxaline *N*-oxide **2s**. The trifluoromethyl-substituted alkynes worked well and highly selectively afforded the corresponding trifluoromethyl-substituted quinoxaline *N*-oxides **2t** and **2u** in moderate yields.

Unfortunately, the electron-deficient anilines did not work well, presumably because of the slow initial hydroamination step under the standard conditions. To expand the substrate scope, we chose the enamine intermediate as substrate and raised the temperature to improve the activity of the intermediates (Figure 3; see also Figures S75–S86). In this way, electron-withdrawing groups, such as ester and carbonyl groups, were well tolerated under the new conditions (**2v** and **2w**). Moreover, the phenyl-substituted alkynes also performed well under these conditions and afforded the corresponding quinoxaline *N*-oxides in moderate yields (**2x–2aa**).

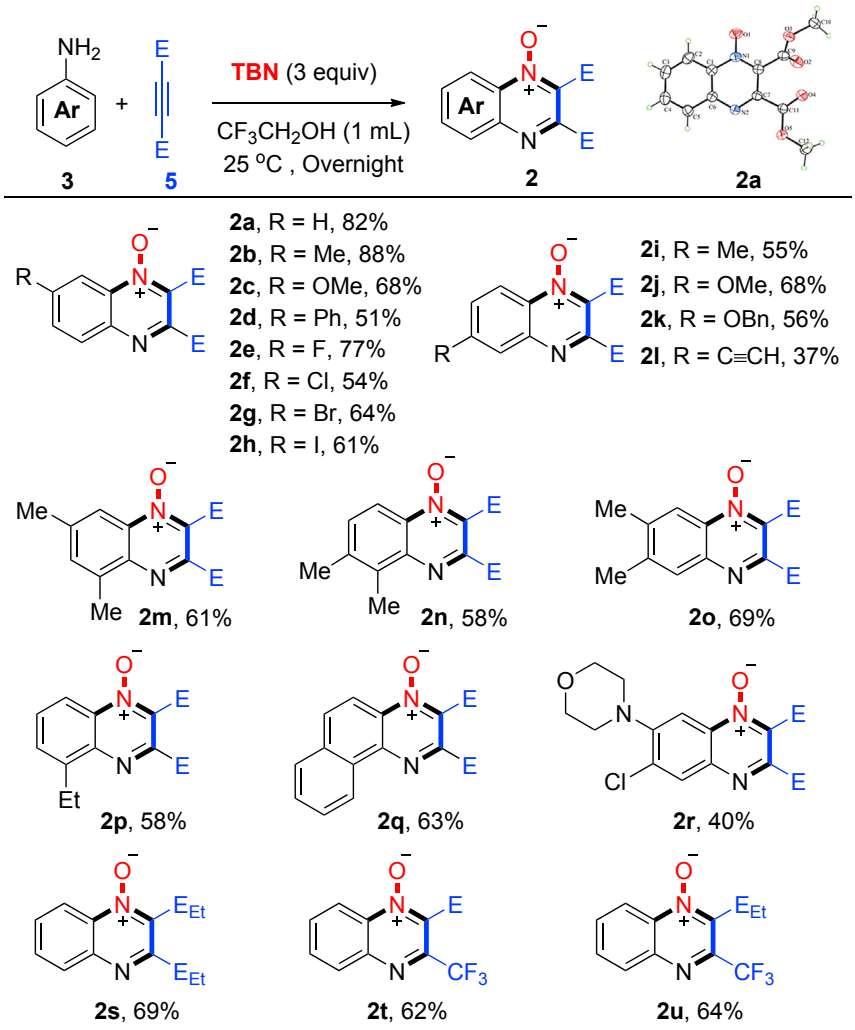

Figure 2. Substrate Scope of Anilines and Electron-Withdrawing Alkynes

For the reaction conditions, see entry 8 in Table 1. The yields are isolated yields based on the aniline substrates. E = CO_2Me, E_{Et} = CO_2Et.

Potential Application in the Synthesis of Bioactive Molecules

To illustrate the practicality of this reaction, we then conducted a gram-scale experiment under the standard conditions, and the desired products 2,5-dihydrooxazole **8b** and quinoxaline *N*-oxide **2b** were obtained in 69% and 81% yield, respectively. The products were isolated by direct recrystallization from the reaction mixture without any routine work-up procedure or column chromatography (equations 1 and 2 in Figure 4).

The products could be deoxidized into quinoxaline derivatives (**10a** and equation 3 in Figure 4; see also Figures S89 and S90). The hydrolysis of the products worked smoothly and the corresponding products were isolated through filtration (**10b** and equation 3 in Figure 4; see also Figures S91 and S92). The *N*-nitrosamines **8b** can also be deprotected under a H_2 atmosphere with Pd/C as the catalyst to deliver **10c** in moderate yield (**10c** and equation 4 in Figure 4; see also Figures S93 and S94). The NO moiety attached to the N atom in the **8b** could also transfer and then be oxidized, realizing the formal nitration of the aromatic ring to provide **10d** (equation 4 in Figure 4; see also Figures S95 and S96).

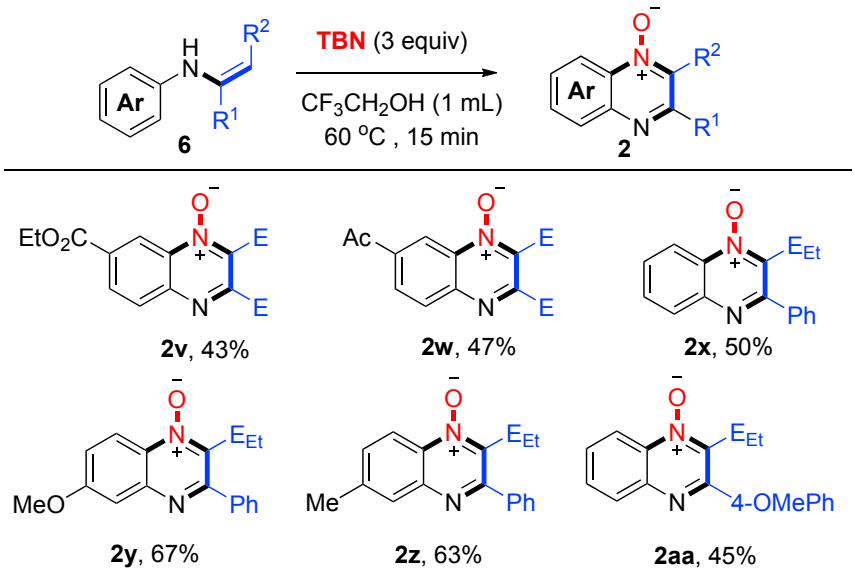

Figure 3. Expansion of the Substrate Scope

Reaction conditions: **6** (0.5 mmol), CF_3CH_2OH (1 mL), stirred at 60°C for 15 min. The yields are isolated yields based on the aniline substrates. E = CO_2Me, E_{Et} = CO_2Et.

Morpholinyl-substituted quinoxaline *N*-oxide **11** with trypanocidal activity was obtained in 43% yield (equation 5 in Figure 5; see also Figures S97 and S98).[52] The saccharide skeleton attached to anilines was also well compatible in this reaction (equation 6 in Figure 5; see also Figures S99 and S100). Decoration of aminoglutethimide, a kind of aromatase inhibitor, also went smoothly to afford **13** in 66% yield (equation 7 in Figure 5; see also Figures S101 and S102). Moreover, the products could be easily converted to antibacterial activity compounds **14** (equation 8 in Figure 5).[53,54] In addition, another two classes of novel structural motif isoxazolo[4,5-*b*] quinoxaline 9-oxides **15** and 1,2,3-triazole 2-oxides **9**, confirmed by X-ray single-crystal diffraction, were discovered (equations 9 and 10 in Figure 5; see also Figures S87, S88, S103, S104, S116, and S117). Constructing fused tricyclic compounds and the special triazole 2-oxides from simple substrates in only one step and incorporating multiple heteroatoms into one ring make this strategy highly efficient and practical.

To gain further insight into the mechanism of the transformation of *N*-methylanilines, we conducted control experiments. The enamine **7a** was isolated in 99% yield under condition B without TBN (equation 11 in Figure 6; see also Figures S107 and S108). The desired product **8a** was obtained in 71% yield with the formed enamine **7a** as the substrate under the optimized conditions, which demonstrates that enamine is involved in this transformation. A labeling experiment with *N*-(methyl-d_3)aniline **4a**-d_3 revealed that methyl shift may proceed via the cleavage of C–N and the formation of C–O and C–N (equation 12 in Figure 6; see also Figures S3 and S4). A cross-labeling experiment showed that methyl shift proceeded in an intermolecular process (equation 13 in Figure 6).

Alternatively, to further explore the mechanism for quinoxaline *N*-oxide formation, we designed and performed another set of control experiments . The enamine **6a** was isolated in 97% yield under condition A without TBN (equation 14 in Figure 6; see also Figures S105 and S106). This provided the desired quinoxaline *N*-oxide **2a** in 83% yield under the optimized conditions (equation 14 in Figure 6), which demonstrates that the enamine was involved in this transformation. Interestingly, the oxime compound **16**

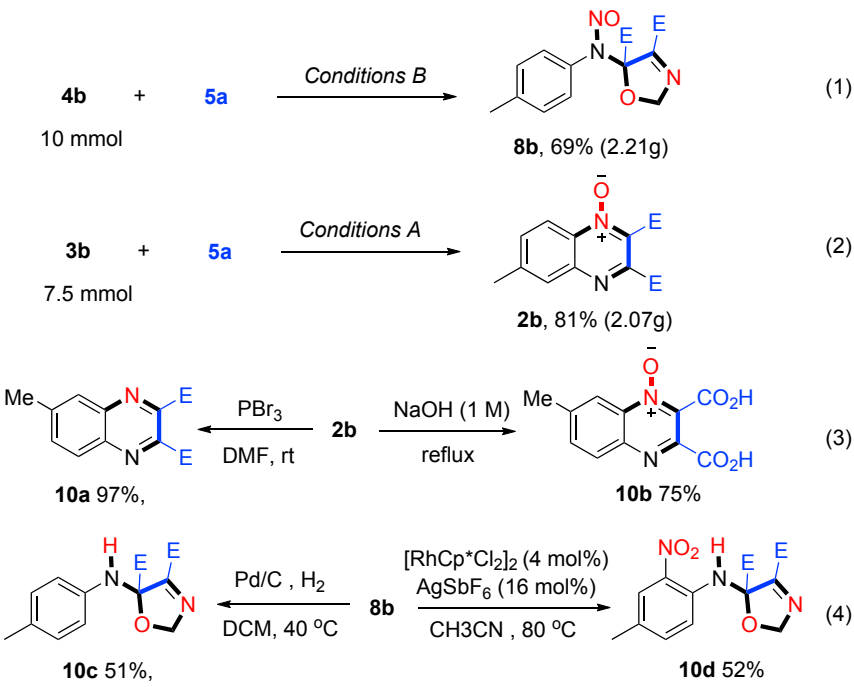

Figure 4. Gram-Scale Experiments and Further Transformations

was isolated in 68% yield in the reaction of **6c** at room temperature, which was confirmed by X-ray single-crystal diffraction (equation 15 in Figure 6; see also Figures S109, S110, and S118). When the formed oxime **16** was used in this transformation, the desired product **2x** was obtained in 70% yield (equation 16 in Figure 6). These results demonstrate that the oxime intermediates and their tautomerism nitroso-substituted imines are most likely the key intermediates of this transformation.

Furthermore, when the reaction of aniline **3a** and alkyne **5a** was monitored by electron paramagnetic resonance (EPR) spectroscopy in the presence of the free radical spin-trapping agent 5,5-dimethyl-1-pyrroline *N*-oxide (DMPO), a signal with six peaks (g = 2.007, αN = 15.5 G, αHβ = 23.6 G; Scheme 2A; see also Figure S111), corresponding to a carbon-centered radical[55] was observed. In addition, the calculated hyperfine splittings of this signal are approximately equal to the reported values[44] (g = 2.011, αN = 15.3 G, αHβ = 22.4 G), indicating that both carbon-centered radicals mainly belong to the same type of carbon-centered radical adjacent to the C=N group. However, the signal did not appear in the absence of TBN (Scheme 2B; see also Figure S112) or the substrates (Scheme 2C; see also Figure S113). These results indicate that the C-centered radical (**A**, Scheme 1C), which is most likely a key intermediate, instead of the N-centered radical (**A′**, Scheme 1C) was involved in the reaction of aniline **3a** and alkyne **5a** with TBN. However, no signal appeared in the reaction of *N*-methylaniline **4a** and alkyne **5a** with TBN under condition B, indicating that pathway b (Scheme 3) is different from pathway a (Scheme 3).

On the basis of all these results and previous reports, a proposed mechanism is depicted in Scheme 3. The reasonable initial step of this transformation is the formation of enamine intermediate **6/7**, as well as the hemolysis of TBN, to generate the *tert*-butoxy radical and NO radical. For the reaction of anilines **3**, H abstraction of the N–H bond by *tert*-butoxy radical occurs to generate radical intermediate **A**, which undergoes radical coupling with the NO radical to afford the nitroso intermediate

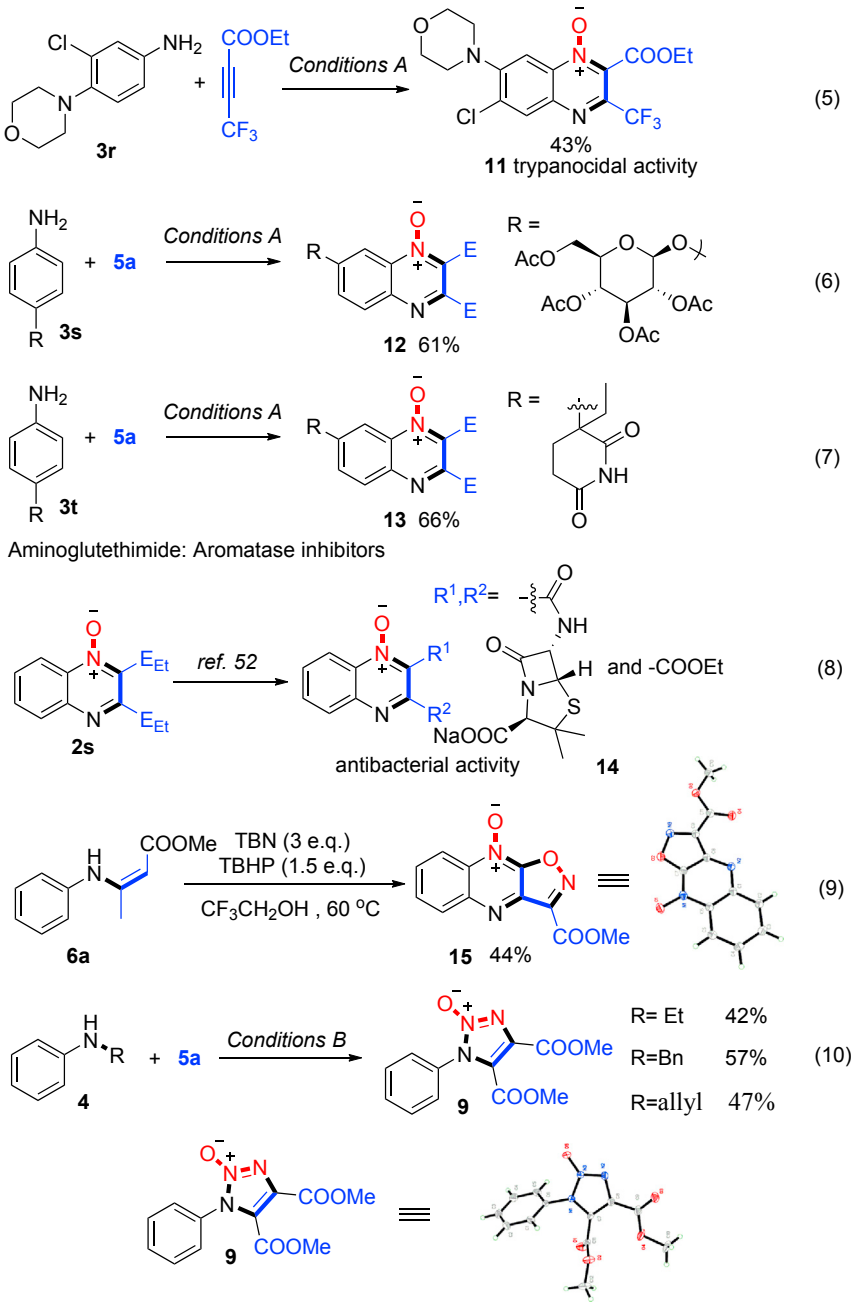

Figure 5. Potential Applications and More Transformations

B. The nitroso intermediate B further undergoes H abstraction to produce radical intermediate C. The cyclic intermediate D is then generated by the subsequent cyclization of C. Finally, aromatization of D through radical H abstraction by the *tert*-butoxy radical leads to the final product 2.

For *N*-methylaniline involved in pathway b, the presence of the *N*-methyl substituent blocks H abstraction without the N–H bond. Then, single-electron oxidation of enamine intermediate 7 occurs to provide radical cation F, which can be further trapped by NO radicals to afford iminium ion G. Then, deprotonation is preferred followed by cyclization to form the four-membered ring I.[56,57] The ring-opening

Please cite this article in press as: Pan et al., Chemoselective Nitrosylation of Anilines and Alkynes via Fragmentary or Complete NO Incorporation, Chem (2018), https://doi.org/10.1016/j.chempr.2018.03.008

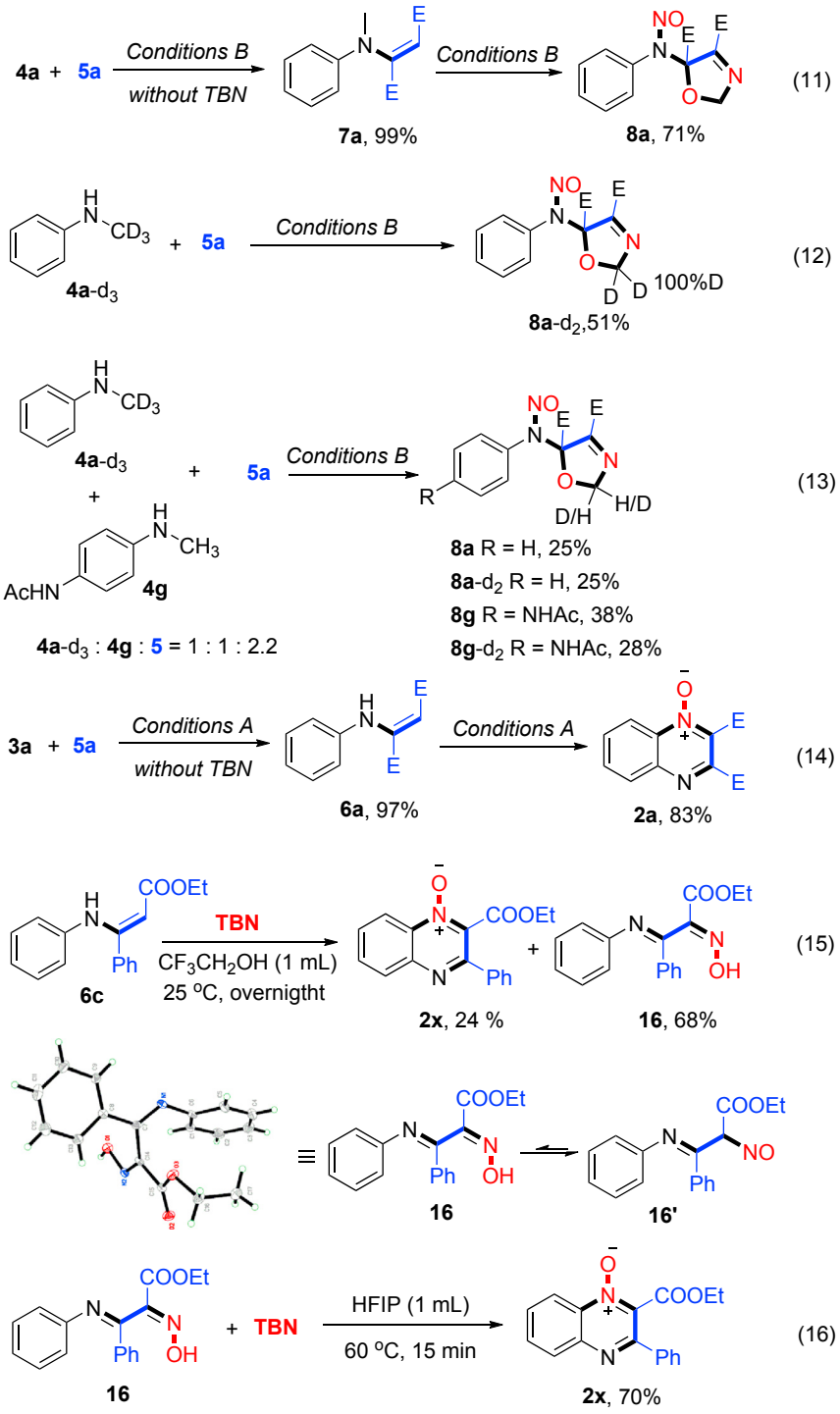

Figure 6. Mechanistic Studies

reaction of I can then occur to afford diradical intermediate J,[36,37] which undergoes an intermolecular methyl shift process with intermediate I or L to form intermediate K. The cyclization of intermediate K with the assistance of tBuO$^-$ produces species L, which undergoes another intermolecular methyl shift process to give intermediate M. Further nitrosylation affords the final product 8.

Please cite this article in press as: Pan et al., Chemoselective Nitrosylation of Anilines and Alkynes via Fragmentary or Complete NO Incorporation, Chem (2018), https://doi.org/10.1016/j.chempr.2018.03.008

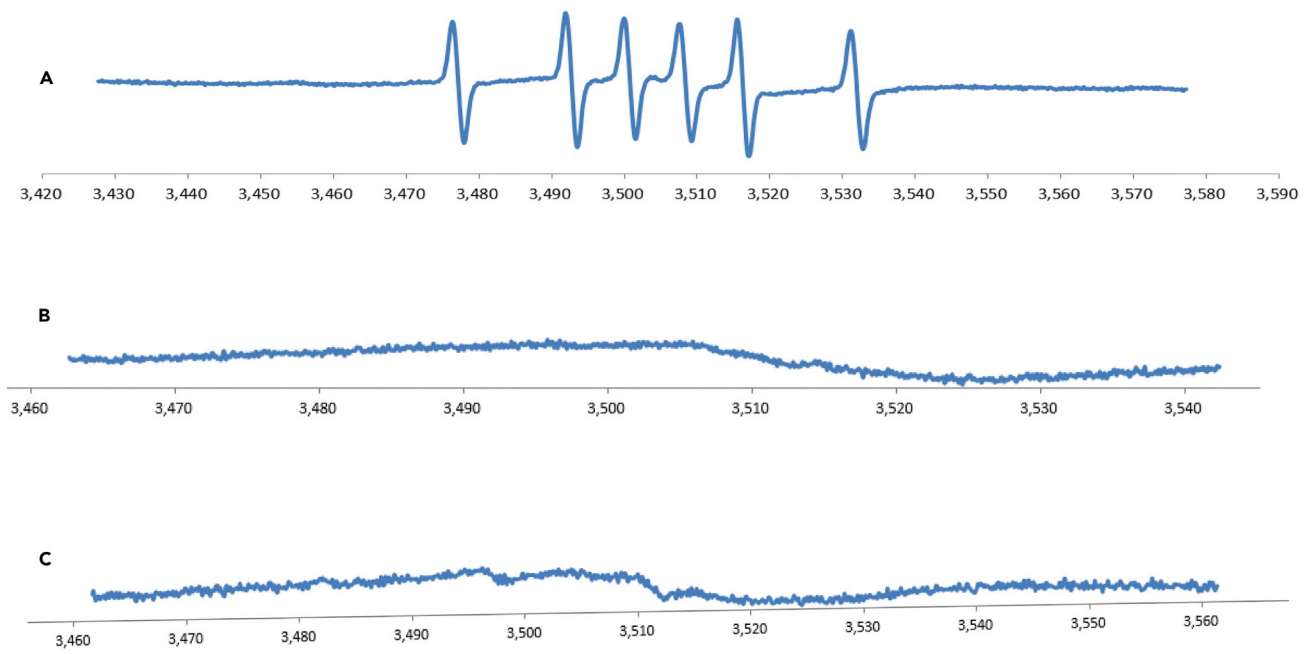

Scheme 2. Electron Paramagnetic Resonance Studies of the Transformation

The EPR spectra (X band, 9.7 GHz, room temperature) in the presence of the radical trap DMPO (2.5×10^{-2} M) at room temperature. (A) **3a** (0.5 mmol), **5a** (0.55 mmol), TBN (1.5 mmol), and CF_3CH_2OH (1 mL) with stirring at 60°C under air for 30 s; (B) without TBN; (C) without **3a** and **5a**.

To better understand this metal-free [3 + 2 + 1] C–H cyclization, we performed preliminary density functional theory (DFT) calculations to investigate the model reaction of aniline **3a** and alkyne **5a** with TBN (Figure 7; for more details, see Figure S119 and Table S3).[58] We propose that the reaction begins with homolysis of TBN into the NO radical and *tert*-butoxy radical,[39,40,59,60] which is endergonic by 22.4 kcal/mol. The cascade annulation reaction initiates into hydroamination of alkyne **5a** as an exothermic step by 18.7 kcal/mol to provide stable enamine **6a**. Then, the abstraction of a hydrogen atom in the N–H bond of **6a** by *in-situ*-formed *tert*-butoxy radical via transition state **TS1a** with an activation free energy of 16.1 kcal/mol afforded radical intermediate **INT1**, which is an irreversible process. The **INT1** formed undergoes radical coupling with the NO radical to form intermediate **INT2**, which is slightly endergonic by 2.9 kcal/mol. Further abstraction of a hydrogen atom in the C–H bond of **INT2** by *tert*-butoxy radical is facile by overcoming the free-energy barrier of 18.8 kcal/mol. This process is significantly exoergic by 77.9 kcal/mol. The following electrocyclic reaction of **INT3** readily proceeds through **TS3** with only an activation free energy of 16.7 kcal/mol to furnish cyclic intermediate **INT4**. Finally, the aromatization process involving the abstraction of a hydrogen atom in **INT4** by *tert*-butoxy radical affords the final quinoxaline *N*-oxide **2a** by releasing a large amount of energy, 149.0 kcal/mol. DFT calculations suggest that the *tert*-butoxy radical and NO radical are the active species. The first abstraction of a hydrogen atom in the N–H bond of **6a** by *tert*-butoxy radical is the rate-determining step, and the subsequent electrocyclic reaction of a radical intermediate serves as the key step, in good agreement with the experimental observations.

The pyrolysis of *tert*-butoxy radical through **TS0** requires a free-energy barrier of 31.7 kcal/mol to give methyl radical with the release of acetone. Although the methyl radical is more stable by 14.4 kcal/mol than the *tert*-butoxy radical, H abstraction by methyl radical was calculated to be unfavorable (Figure 7).

Please cite this article in press as: Pan et al., Chemoselective Nitrosylation of Anilines and Alkynes via Fragmentary or Complete NO Incorporation, Chem (2018), https://doi.org/10.1016/j.chempr.2018.03.008

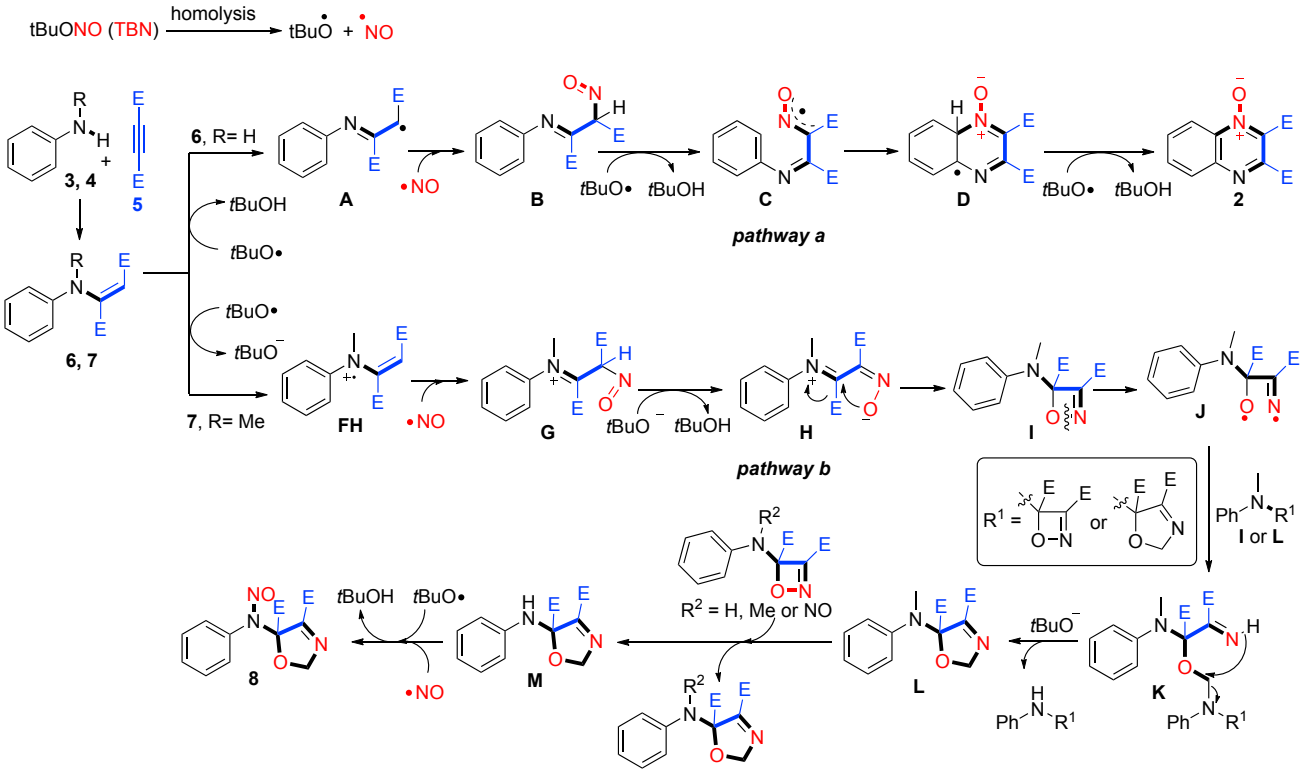

Scheme 3. Proposed Mechanism

The DFT calculations on the reaction of *N*-methylaniline (**4a**) and alkyne **5a** showed that the first step corresponds to hydroamination of alkyne **5a** as an exothermic step by 12.8 kcal/mol to provide stable enamine **7a** (Figure 8; for more details, see the Supplemental Information). Then single-electron oxidation of enamine intermediate **7a** occurs to provide radical cation intermediate **INT5**, which requires a free energy of 27.4 kcal/mol. The further capture by NO radicals is slightly

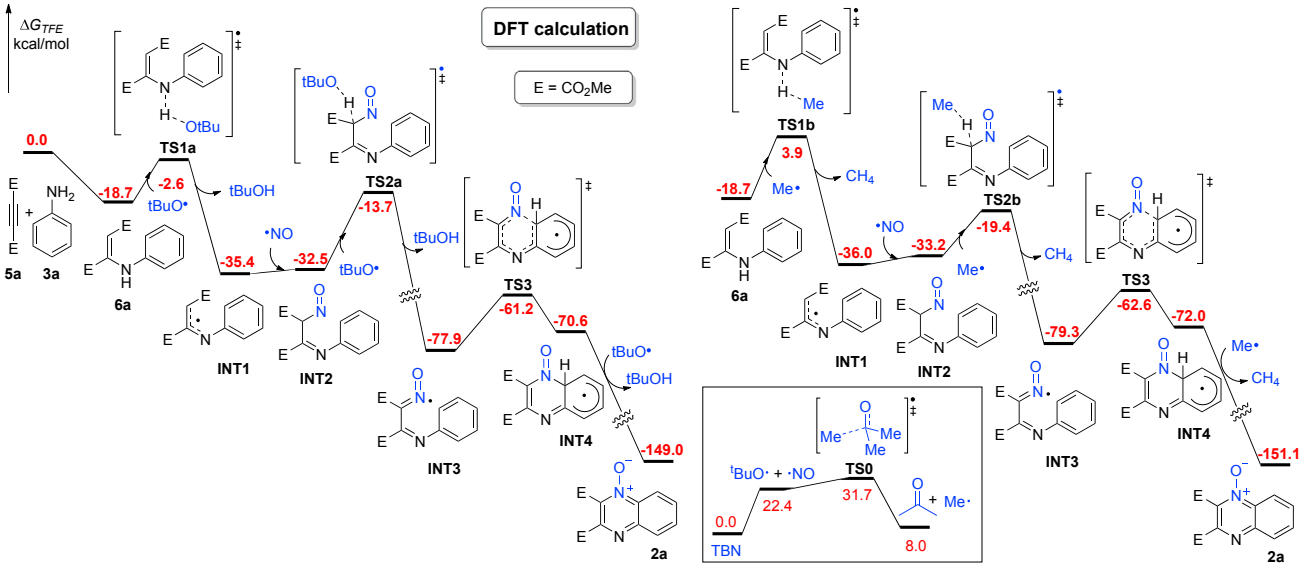

Figure 7. DFT-Computed Energy Profiles for the *N*-Incorporation Reaction of Aniline 3a and Alkyne 5a with TBN

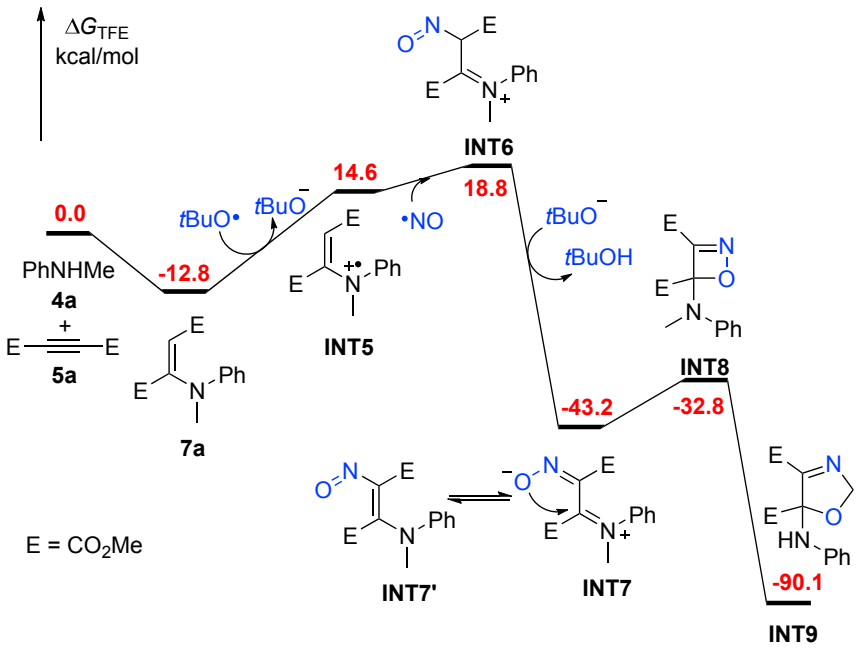

Figure 8. DFT-Computed Energy Profiles for the *N,O*-Incorporation Reaction of Aniline 4a and Alkyne 5a with TBN

endergonic by 4.2 kcal/mol to afford imine cation **INT6**. Then, deprotonation by *tert*-butoxy anion is preferred to provide **INT7**, which is significantly exothermic. The following cyclization of **INT7** requires a free energy of 10.4 kcal/mol to form the four-membered ring **INT8**. The ring-opening reaction of **INT8** can occur to afford a diradical intermediate, which undergoes an intramolecular or intermolecular methyl shift exothermic process to form intermediate **INT9**. Finally, the abstraction of a hydrogen atom in the N–H bond followed by radical coupling with the NO radical affords the product **8a**.

In conclusion, we have developed a chemoselective nitrosylation of anilines and alkynes for the efficient construction of 2,5-dihydrooxazoles, 1*H*-1,2,3-triazole 2-oxides, and quinoxaline *N*-oxides through fragmentary or complete NO radical incorporation. C–H bond cleavage, the formation of multiple C–N bonds, unexpected C–N bond cleavage, and N=O bond cleavage are involved in this chemistry. Facile operation in open-air, metal-free, and mild conditions at room temperature or 60°C makes this protocol particularly practical and attractive. A reasonable mechanism consistent with labeling experiments, isolation of the intermediates, DFT calculations, and EPR measurements is provided. Further studies to design new reactions and synthetic applications are ongoing in our laboratory.

EXPERIMENTAL PROCEDURES

Representative Procedure for the Complete Incorporation Approach to Quinoxaline *N*-Oxides

To a 10 mL Schlenk flask containing anilines **3** (0.5 mmol), electron-withdrawing alkynes **5** (0.55 mmol) were added and then the flask allowed to stand for 5 min. A magnetic stir bar and CF_3CH_2OH (1 mL) were added to the mixture and stirred for 2 min. TBN (1.5 mmol) was then added to the mixture in 10 s, and the mixture was plugged and stirred at 25°C overnight. The reaction mixture was diluted with AcOEt,

and the solution was concentrated under vacuum. Finally, the mixture was purified through column chromatography to afford the pure products **2**.

Representative Procedure for the Fragmentary Cycloaddition Approach to 2,5-Dihydrooxazoles

To a 10 mL Schlenk flask containing *N*-methylanilines **4** (0.5 mmol), electron-withdrawing alkynes **5** (0.55 mmol) were added and the flask was allowed to stand for 5 min. A magnetic stir bar and HFIP (1 mL) were added to the mixture and stirred at 60°C for 2 min. TBN (1.1 mmol) was then added to the mixture in 10 s, and the mixture was plugged and stirred at 60°C for 15 min. The reaction mixture was diluted with AcOEt and the solution was concentrated under vacuum. Finally, the mixture was purified through column chromatography to afford the pure products **8**.

DATA AND SOFTWARE AVAILABILITY

The data for the X-ray crystallographic structures of products **2a**, **8h**, **9**, **15**, and **16** in this article have been deposited in the Cambridge Crystallographic Data Center under accession numbers CCDC: 1828890, 1828891, 1828892, 1828893, and 1828894, respectively.

SUPPLEMENTAL INFORMATION

Supplemental Information includes Supplemental Experimental Procedures, 119 figures, 3 tables, and 5 data files and can be found with this article online at https://doi.org/10.1016/j.chempr.2018.03.008.

ACKNOWLEDGMENTS

Financial support from the National Natural Science Foundation of China (nos. 21632001 and 21772002), National Basic Research Program of China (973 Program) (grant no. 2015CB856600), National Young Top-notch Talent Support Program, and Peking University Health Science Center (no. BMU20160541) is greatly appreciated. We thank Hao Wu in this group for reproducing the results of **2u** and **2aa**. This work is dedicated to Professor Jin-Pei Cheng on the occasion of his 70th birthday.

AUTHOR CONTRIBUTIONS

J.P., X.L., and N.J. conceived and designed the experiments; J.P. carried out most of the experiments; X.L. carried out most of the calculations; J.P., X.L., and N.J. analyzed the data; F.L. and J.L. carried out some experiments; J.P., X.L., and N.J., wrote the paper; N.J. directed the project.

DECLARATION OF INTERESTS

The authors declare no competing financial interests.

Received: August 4, 2017
Revised: November 19, 2017
Accepted: March 11, 2018
Published: April 19, 2018

REFERENCES AND NOTES

1. Alcaide, B., Almendros, P., and Aragoncillo, C. (2010). Exploiting [2+2] cycloaddition chemistry: achievements with allenes. Chem. Soc. Rev. *39*, 783–816.

2. Xu, X., and Doyle, M.P. (2014). The [3 + 3]-cycloaddition alternative for heterocycle syntheses: catalytically generated metalloenolcarbenes as dipolar adducts. Acc. Chem. Res. *47*, 1396–1405.

3. Chen, J.R., Hu, X.Q., Lu, L.Q., and Xiao, W.J. (2015). Formal [4+1] annulation reactions in the synthesis of carbocyclic and heterocyclic systems. Chem. Rev. *115*, 5301–5365.

4. Appukkuttan, P., Mehta, V.P., and Van der Eyken, E. (2010). V. Microwave-assisted cycloaddition reactions. Chem. Soc. Rev. *39*, 1467–1477.

5. Masson, G., Lalli, C., Benohoud, M., and Dagousset, G. (2013). Catalytic enantioselective [4 + 2]-cycloaddition: a strategy to access aza-hexacycles. Chem. Soc. Rev. *42*, 902–923.

6. Yeom, H.S., and Shin, S. (2014). Catalytic access to α-Oxo gold carbenes by N–O bond oxidants. Acc. Chem. Res. *47*, 966–977.

7. Shi, Z., and Glorius, F. (2012). Efficient and versatile synthesis of indoles from enamines and imines by cross-dehydrogenative coupling. Angew. Chem. Int. Ed. *51*, 9220–9222.

8. Waser, M., and Novacek, J. (2015). An organocatalytic biomimetic strategy paves the way for the asymmetric umpolung of imines. Angew. Chem. Int. Ed. *54*, 14228–14231.

9. Chiba, S. (2013). Cu-catalyzed aerobic molecular transformation of imine and enamine derivatives for synthesis of azaheterocycles. Bull. Chem. Soc. Jpn. *86*, 1400–1411.

10. Yu, J., Shi, F., and Gong, L.Z. (2011). Brønsted-acid-catalyzed asymmetric multicomponent reactions for the facile synthesis of highly enantioenriched structurally diverse nitrogenous heterocycles. Acc. Chem. Res. *44*, 1156–1171.

11. Hummel, J.R., Boerth, J.A., and Ellman, J.A. (2017). Transition-metal-catalyzed C–H bond addition to carbonyls, imines, and related polarized π bonds. Chem. Rev. *117*, 9163–9227.

12. Klier, L., Tur, F., Poulsen, P.H., and Jørgensen, K.A. (2017). Asymmetric cycloaddition reactions catalysed by diarylprolinol silyl ethers. Chem. Soc. Rev. *46*, 1080–1102.

13. Mukherjee, S., Yang, J.W., Hoffmann, S., and List, B. (2007). Asymmetric enamine catalysis. Chem. Rev. *107*, 5471–5569.

14. Cheng, D., Ishihara, Y., Tan, B., and Barbas, C.F., III (2014). Organocatalytic asymmetric assembly reactions: synthesis of spirooxindoles via organocascade strategies. ACS Catal. *4*, 743–762.

15. Akiyama, T., and Mori, K. (2015). Stronger Brønsted acids: recent progress. Chem. Rev. *115*, 9277–9306.

16. Brak, K., and Jacobsen, E.N. (2013). Asymmetric ion-pairing catalysis. Angew. Chem. Int. Ed. *52*, 534–561.

17. Li, J.L., Liu, T.Y., and Chen, Y.C. (2012). Aminocatalytic asymmetric Diels–Alder reactions via HOMO activation. Acc. Chem. Res. *45*, 1491–1500.

18. Phipps, R.J., Hamilton, G.L., and Toste, F.D. (2012). The progression of chiral anions from concepts to applications in asymmetric catalysis. Nat. Chem. *4*, 603–614.

19. MacMillan, D.W.C. (2008). The advent and development of organocatalysis. Nature *455*, 304–308.

20. Schiesser, C.H., Wille, U., Matsubara, H., and Ryu, I. (2007). Radicals masquerading as electrophiles: dual orbital effects in nitrogen-philic acyl radical cyclization and related addition reactions. Acc. Chem. Res. *40*, 303–313.

21. Kumar, I., Ramaraju, P., and Mir, N.A. (2013). Asymmetric trienamine catalysis: new opportunities in amine catalysis. Org. Biomol. Chem. *11*, 709–716.

22. Nicolaou, K.C., Reingruber, R., Sarlah, D., and Brase, S. (2009). Enantioselective intramolecular Friedel–Crafts-type α-arylation of aldehydes. J. Am. Chem. Soc. *131*, 2086–2087.

23. Hick-man, A.J., and Sanford, M.S. (2012). High-valent organometallic copper and palladium in catalysis. Nature *484*, 177–185.

24. Davies, H.M., and Manning, J.R. (2008). Catalytic C–H functionalization by metal carbenoid and nitrenoid insertion. Nature *451*, 417–424.

25. Yeung, C.S., and Dong, V.M. (2011). Catalytic dehydrogenative cross-coupling: forming carbon–carbon bonds by oxidizing two carbon–hydrogen bonds. Chem. Rev. *111*, 1215–1292.

26. Colby, D.A., Bergman, R.G., and Ellman, J.A. (2010). Rhodium-catalyzed C–C bond formation via heteroatom-directed C–H bond activation. Chem. Rev. *110*, 624–655.

27. Delord, J.-W., Droge, T., Liu, F., and Glorius, F. (2011). Towards mild metal-catalyzed C–H bond activation. Chem. Soc. Rev. *40*, 4740–4761.

28. Souillart, L., and Cramer, N. (2015). Catalytic C–C bond activations via oxidative addition to transition metals. Chem. Rev. *115*, 9410–9464.

29. Dermenci, A., Coe, J.W., and Dong, G. (2014). Direct activation of relatively unstrained carbon–carbon bonds in homogeneous systems. Org. Chem. Front. *1*, 567–581.

30. Tobisu, M., and Chatani, N. (2008). Catalytic reactions involving the cleavage of carbon–cyano and carbon–carbon triple bonds. Chem. Soc. Rev. *37*, 300–307.

31. Jun, C.H. (2004). Transition metal-catalyzed carbon–carbon bond activation. Chem. Soc. Rev. *33*, 610–618.

32. Ishida, N., Sawano, S., and Murakami, M. (2014). Stereospecific ring expansion from orthocyclophanes with central chirality to metacyclophanes with planar chirality. Nat. Commun. *5*, 3111–3119.

33. Masarwa, A., Weber, M., and Sarpong, R. (2015). Selective C–C and C–H bond activation/cleavage of pinene derivatives: synthesis of enantiopure cyclohexenone scaffolds and mechanistic insights. J. Am. Chem. Soc. *137*, 6327–6334.

34. Ishida, N., Ikemoto, W., and Murakami, M. (2014). Cleavage of C–C and C–Si σ-bonds and their intramolecular exchange. J. Am. Chem. Soc. *136*, 5912–5915.

35. Xu, Z., Zhang, C., and Jiao, N. (2012). Synthesis of oxazoles through copper-mediated aerobic oxidative dehydrogenative annulation and oxygenation of aldehydes and amines. Angew. Chem. Int. Ed. *51*, 11367–11370.

36. Zhang, C., Xu, Z.J., Zhang, L.J., and Jiao, N. (2011). Copper-catalyzed aerobic oxidative coupling of aryl acetaldehydes with anilines leading to α-ketoamides. Angew. Chem. Int. Ed. *50*, 11088–11092.

37. Zhang, C., and Jiao, N. (2010). Dioxygen activation under ambient conditions: Cu-catalyzed oxidative amidation–diketonization of terminal alkynes leading to α-ketoamides. J. Am. Chem. Soc. *132*, 28–29.

38. Chen, F., Huang, X., Cui, Y., and Jiao, N. (2013). Direct transformation of methyl imines to α-iminonitriles under mild and transition-metal-free conditions. Chem. Eur. J. *19*, 11199–11202.

39. Hirabayashi, T., Sakaguchi, S., and Ishii, Y. (2004). A new route to lactam precursors from cycloalkanes: direct production of nitrosocycloalkanes or cycloalkanone oximes by using tert-butyl nitrite and N-hydroxyphthalimide. Angew. Chem. Int. Ed. *43*, 1120–1123.

40. Shu, Z., Ye, Y., Deng, Y., Zhang, Y., and Wang, J. (2013). Palladium(II)-catalyzed direct conversion of methyl arenes into aromatic nitriles. Angew. Chem. Int. Ed. *52*, 10573–10576.

41. Liu, J., Zheng, H.X., Yao, C.Z., Sun, B.F., and Kang, Y.B. (2016). Pharmaceutical-oriented selective synthesis of mononitriles and dinitriles directly from methyl(hetero)arenes: access to chiral nitriles and citalopram. J. Am. Chem. Soc. *138*, 3294–3297.

42. Liang, Y.-F., Li, X., Wang, X., Yan, Y., Feng, P., and Jiao, N. (2015). Aerobic oxidation of PdII to PdIV by active radical reactants: direct C–H nitration and acylation of arenes via oxygenation process with molecular oxygen. ACS Catal. *5*, 1956–1963.

43. Liu, Y., Zhang, J.L., Song, R.J., Qian, P.C., and Li, J.H. (2014). Cascade nitration/cyclization of 1,7-enynes with tBuONO and H_2O: one-pot self-assembly of pyrrolo[4,3,2-de]quinolinones. Angew. Chem. Int. Ed. *53*, 9017–9020.

44. Chen, F., Huang, X., Li, X., Shen, T., Zou, M., and Jiao, N. (2014). Dehydrogenative N-incorporation: a direct approach to quinoxaline N-oxides under mild conditions. Angew. Chem. Int. Ed. *53*, 10495–10499.

45. Mfuh, A.M., Nguyen, V.T., Chhetri, B., Burch, J.E., Doyle, J.D., Nesterov, V.N., Arman, H.D., and Larionov, O.V. (2016). Additive- and metal-free, predictably 1,2- and 1,3-regioselective, photoinduced dual C–H/C–X borylation of haloarenes. J. Am. Chem. Soc. *138*, 8408–8411.

46. Glinkerman, C.M., and Boger, D.L. (2016). Catalysis of heterocyclic azadiene cycloaddition reactions by solvent hydrogen bonding: concise total synthesis of methoxatin. J. Am. Chem. Soc. *138*, 12408–12413.

47. Ouyang, K., Hao, W., Zhang, W.X., and Xi, Z. (2015). Transition-metal-catalyzed cleavage of C–N single bonds. Chem. Rev. *115*, 12045–12090.

48. Wang, Q., Su, Y., Li, L., and Huang, H. (2016). Transition-metal catalysed C–N bond activation. Chem. Soc. Rev. *45*, 1257–1272.

49. Desnoyer, A.N., and Love, J.A. (2017). Recent advances in well-defined, late transition metal

complexes that make and/or break C–N, C–O and C–S bonds. Chem. Soc. Rev. *46*, 197–238.

50. Wan, X.-B. (2014). Homogeneous transition-metal catalyzed C–N activation. In Homogeneous Catalysis for Unreactive Bond Activation, Z.-J. Shi, ed. (John Wiley), pp. 269–316.

51. Wang, R., and Falck, J.R. (2014). Transformations of X (C, O, N)–CN bonds: cases of selective X (C, O, N)–C activation. RSC Adv. *4*, 1062–1066.

52. Pérez-Silanes, S., Torres, E., Arbillaga, L., Varela, J., Cerecetto, H., Gonzalez, M., Azqueta, A., and Moreno-Viguri, E. (2016). Synthesis and biological evaluation of quinoxaline di-N-oxide derivatives with in vitro trypanocidal activity. Bioorg. Med. Chem. Lett. *26*, 903–906.

53. Edwards, M.L., Bambury, R.E., and Ritter, H.W. (1976). Beta-Lactam antibiotics with N-oxide side chains. 1. Quinoxaline N-oxides. J. Med. Chem. *19*, 330–333.

54. Carmeli, M., and Rozen, S. (2006). A new efficient route for the formation of quinoxaline N-oxides and N,N′-dioxides using HOF·CH_3CN. J. Org. Chem. *71*, 5761–5765.

55. Hardy, M., Ouari, O., Charles, L., Finet, J.-P., Iacazio, G., Monnier, V., Rockenbauer, A., and Tordo, P. (2005). Synthesis and spin-trapping behavior of 5-ChEPMPO, a cholesteryl ester analogue of the spin trap DEPMPO. J. Org. Chem. *70*, 10426–10433.

56. Wieser, K., and Berndt, A. (1975). Stabile 4H-1,2-Oxazete durch intramolekulare Cyclisierung α,β-ungesättigter Nitrosoverbindungen. Angew. Chem. *87*, 73–74.

57. Durchschein, K., Fabian, W.M., Macheroux, P., Zangger, K., Trimmel, G., and Faber, K. (2011). Reductive biotransformation of nitroalkenes via nitroso-intermediates to oxazetes catalyzed by xenobiotic reductase A (XenA). Org. Biomol. Chem. *9*, 3364–3369.

58. Computational details and references are given in the Supplemental Information.

59. Miao, C.-X., Yu, B., and He, L.-N. (2011). Tert-butyl nitrite: a metal-free radical initiator for aerobic cleavage of benzylic C=C bonds in compressed carbon dioxide. Green Chem. *13*, 541–544.

60. Effenhauser, C.S., Felder, P., and Huber, J.R. (1990). Photodissociation of alkyl nitrites in a molecular beam. Primary and secondary reactions. J. Phys. Chem. *94*, 296–302.